




Macro-based collagen quantification and segmentation in picosirius red-stained heart sections using light microscopy

Julian Kammerer¹, Alexandra Cirnu ¹, Tatjana Williams¹, Melanie Hasselmeier¹, Mike Nörpel¹, Ruping Chen ¹ and Brenda Gerull ^{1,2,*}

¹Comprehensive Heart Failure Center, Department of Cardiovascular Genetics, University Hospital Würzburg, Würzburg, 97078, Germany

²Department of Medicine I, University Hospital Würzburg, Würzburg, 97078, Germany

*Correspondence address: Comprehensive Heart Failure Center (CHFC) and Department of Medicine I, University Hospital Würzburg, Am Schwarzenberg 15, 97078 Würzburg, Germany. Tel: +49 931 201 46457; E-mail: Gerull_B@ukw.de

Abstract

Picosirius red staining constitutes an important and broadly used tool to visualize collagen and fibrosis in various tissues. Although multiple qualitative and quantitative analysis methods to evaluate fibrosis are available, many require specialized devices and software or lack objectivity and scalability. Here, we aimed to develop a versatile and powerful “QuantSeg” macro in the FIJI image processing software capable of automated, robust, and quick collagen quantification in cardiac tissue from light micrographs. To examine different patterns of fibrosis, an optional segmentation algorithm was implemented. To ensure the method’s validity, we quantified the collagen content in a set of wild-type versus plakoglobin-knockout murine hearts exhibiting extensive fibrosis using both the macro and an established, fluorescence microscopy-based method, and compared results. To demonstrate the capabilities of the segmentation feature, rat hearts were examined post-myocardial infarction. We found the QuantSeg macro to robustly detect the differences in fibrosis between knockout and control hearts. In sections with low collagen content, the macro yielded more consistent results than using the fluorescence microscopy-based technique. With its wide range of output parameters, ease of use, cost effectiveness, and objectivity, the QuantSeg macro has the potential to become an established method for analysis of PSR-stained tissue. The novel segmentation feature allows for automated evaluation of different patterns of cardiac fibrosis for the first time.

Keywords: pico-sirius red; collagen quantification; heart segmentation; macro-based analysis

Introduction

Picosirius red (PSR) is a histological staining technique used to mark collagen fibers in various tissue sections. After early experiments in the 1960s and its proper description in 1979, it has garnered widespread use as a tool to visualize collagen content in different organs and to assess the amount, size, and distribution of fibrotic areas [1–3]. Hallmarks of this technique include the simplicity of its staining procedure, high sensitivity, and specificity based on a strong interaction between collagen and dye, and purported hue and color saturation stability toward fluctuations in staining solution composition as well as overtime [3]. PSR staining was primarily intended to be used in conjunction with polarization microscopy due to the induction of birefringence in collagen fibers, thereby ensuring high specificity as the few non-collagen structures stained red by PSR (such as keratohyalin granules, some fish hearts, and mucous producing cells in some species) are not birefringent or, in the case of amyloid, lack the typical fibrous appearance [2, 3].

However, due to lacking experience with and limited access to polarization microscopy in many institutions, alternative methods of analysis and quantification are frequently used. To date, there is no gold-standard technique of analyzing PSR-stained sections. Apart from polarization microscopy-based detection of

collagen birefringence, available methods include hue-based discrimination of collagen and parenchyma in bright-field images (BF), the employment of physical glass filters blocking part of the color spectrum, and the usage of conventional or confocal fluorescence microscopy [3–5]. Based on those forms of image acquisition, a plethora of ways handling and analyzing the image data exists, including purely qualitative histopathological evaluation, collagen spot counting over a grid, manual pixel-based quantification involving open-source or proprietary image analysis software, and automated approaches such as macros in programs like ImageJ [5–9]. Some of these techniques are plagued by a certain degree of subjectivity which could influence results, be it in estimating and manually setting exposure times or in interpreting what counts as a collagen spot and what does not. Another problem is the time-consuming nature of some methods which often renders them unsuitable for large projects as they are not scalable to hundreds or thousands of images. For computational solutions, frequently, the usage of multiple and sometimes paid programs is required alongside numerous and repetitive user inputs for each image. Regarding the few automated script-based solutions described so far, either the source code has not been made available by the authors, or it is outdated and does not run with modern versions of the respective software [7, 9]. Regardless

Received: 20 March 2024. Revised: 17 April 2024. Editorial decision: 22 April 2024. Accepted: 26 April 2024

© The Author(s) 2024. Published by Oxford University Press.

This is an Open Access article distributed under the terms of the Creative Commons Attribution-NonCommercial License (<https://creativecommons.org/licenses/by-nc/4.0/>), which permits non-commercial re-use, distribution, and reproduction in any medium, provided the original work is properly cited. For commercial re-use, please contact journals.permissions@oup.com

of the underlying microscopy, most computational approaches quantify the collagen amount or degree of fibrosis by only calculating the fractional area of collagen compared to the total tissue area [7–9]. Histochemical approaches such as hydroxyproline assays lack the capability of elucidating the spatial distribution of collagen in the sample yet provide low cost and high scalability [10].

Here, we present a publicly available, free, fully automated, and time-saving method for collagen quantification and localization in PSR-stained histological heart sections, yielding a more comprehensive set of measurements than previous approaches. Furthermore, we aimed to enable a degree of flexibility enabling the method to be used for other samples besides cardiac tissue.

Given that different pathologies lead to different distribution patterns of fibrosis in the heart is not natively accounted for by most analysis techniques, a differentiation of cardiac regions is only possible by manually capturing view frames from the respective areas of interest. Aiming at a more objective and less time-consuming solution, we developed a technique which automatically creates segmentations of whole murine heart sections into different micro-anatomical regions—to then serve as a foundation for subsequent collagen quantification.

Depending on the research question, the here-described novel “QuantSeg” macro can either quantify total collagen amounts within a heart section or automatically perform a comprehensive segmentation into its sub-regions (e.g. epicardium, myocardium, endocardium, etc). The techniques either can be run separately or be combined to obtain collagen quantification in the different micro-anatomical regions of interest.

Materials and methods

In order to meet all the criteria stated above, we decided to develop a macro in FIJI (RRID: SCR_002285) [11]. This versatile image analysis software is a distribution of the program ImageJ2, which is bundled in FIJI with a plethora of plugins and tools [12]. It includes a powerful script editor in which almost all functions of the program can be controlled automatically in conjunction with extensive access to the computer’s file system. The resulting scripts, so-called macros, can be installed and/or run in any program instance of FIJI as long as a suitably up-to-date version is used. The macro was last tested by us in 1.54f from July 2023. It is available at GitHub under the AGPL-3.0 license (<https://doi.org/10.5281/zenodo.10480349>), also linked to within the [supplementary material](#). There, an installation guide, a detailed manual, a video demonstration of QuantSeg’s usage, and the raw data can be found, as well.

Animal models and tissue samples

Heart sections exhibiting substantial amounts of collagen were obtained from two different rodent *in vivo* models. First, we used cardiac tissue from a cardiomyocyte-restricted homozygous plakoglobin-deficient (*Jup*-KO) mouse model which develops a cardiomyopathic phenotype with progressive cardiac dysfunction and cardiac fibrotic remodeling [13]. *Jup*-KO mice were generated as described previously [14, 15].

Analysis was conducted on cardiac tissue from 6- and 8-week-old *Jup*-KO and wild-type (WT) littermate controls of both genders. Secondly, we used heart tissue from rats at 8 weeks after sham surgery or experimental myocardial infarction (MI), the latter of which display segmental, transmural fibrosis. Surgeries were conducted as previously described [16].

All animal handling was in compliance with the directive 2010/63/EU of the European Parliament and was conducted in accordance with institutional guidelines. The animals were housed in a climate-controlled facility on a 12-hour light/dark cycle and offered standard chow and water *ad libitum*.

PSR staining

To evaluate the extent of fibrosis, murine cardiac tissue samples were obtained and treated as previously described [13]. In brief, hearts were excised, fixed in 4% methanol-free formalin (Polysciences Cat# 18814-10) in PBS, embedded in paraffin and transversally sectioned (thickness 20 μ m) using an RM2245 microtome by Leica Biosystems. Prior to staining with PSR, the sections were deparaffinated, rehydrated, washed, and incubated in PSR working solution (Morphisto Cat# 13422) for 25 min. After washing and dehydration, samples were mounted in water-free medium (EntellanTM, Merck Cat# 107960).

Bright-field microscopy

All images within this study were acquired using a BZ-X810 microscope by KEYENCE. Slides were imaged using a 20X objective lens with an exposure time of 1/120 second. After adjusting white balance, tile images were captured at a resolution of 1920*1440 pixels. Finally, using the microscope’s proprietary software, tiles were stitched and saved with and without compression to obtain both a high-resolution overview image as well as a compressed version of lower file size. Using the QuantSeg macro, images were analyzed, first without segmentation to validate the method, and then with segmentation enabled to test the capabilities of this function.

Collagen quantification

To obtain robust collagen quantification values as output parameters, 8-bit BF overview images of heart sections were processed and analyzed using the QuantSeg macro. In brief, each image was split into its hue, saturation, and brightness channels (HSB). The saturation channel was used to create a selection for the background area by applying a brightness threshold. The resulting selection was transferred to the original image to measure the mean red, green, and blue (RGB) values of the background. In case the three obtained values displayed a discrepancy, the whole image’s RGB components were adjusted in order to establish correct white balance. Following that, the background areas were filled in with pure white to ease analysis and publication of the respective image. To differentiate between collagenous and parenchymal areas, the original BF image was transferred into the L*a*b* color space. Parenchyma and collagen selections were created by applying brightness thresholds to the resulting a* and hue channel, respectively. Both selections were transferred to the previously created saturation channel of the HSB color space to individually measure area and mean saturation of the different tissue compartments. For the collagen selection, max gray value, spot count, and mean spot area were measured as additional values. Based on these values the output parameters Collagen Score, Area Fraction, Collagen Area, Mean Collagen Intensity, Max Collagen Intensity, Mean Spot Area, Spot Count, and Tissue Density were calculated and saved as .csv and/or .xlsx-files, the latter of which being only available after segmentation due to technical reasons. A detailed explanation of output values can be found in [Supplementary Table 1](#).

Heart segmentation

Automatic segmentation of heart sections was developed for and tested with murine tissue. Starting from continuous overview micrographs of transverse heart sections, the tissue silhouette was determined by recognizing two non-connected and continuously bordered holes, interpreted as ventricle lumina. In case this pre-requisite was not given in the present tissue section, the *QuantSeg* macro was programmed to enable manual input for assisting feature recognition. Following the identification of the heart silhouette and the ventricle lumina, regions of interest (ROIs) were fitted to those structures and subsequently used to construct the remaining region ROIs. For heart segmentation by wall layers, the silhouette ROI was shrunk by a pre-defined value and subtracted from the original ROI to obtain a ring-like ROI for the epicardium. Endocardial ROIs were constructed in a similar manner by enlarging the ventricle lumen ROIs, respectively. The adjacent layers—subepi- and subendocardium—were then created by shrinking or enlarging existing ROIs by preset amounts, carefully ensuring not to include background or ventricle lumen. However, in regions with low mural thickness, the same area could be assigned to both subepi- and subendocardium. The remaining areas were defined as a collective myocardial ROI. During the assignment of the different ROIs, discrimination between left and right ventricle was performed, based on the presumption that on average the right ventricular free wall is thinner than the left one. Wall thicknesses were measured by constructing a line through the center points of both ventricles, that is orthogonal to the septal plane. This line was then used to measure the thickness of both opposite free walls at different positions. Afterward, the mean thickness values were compared to take the final decision between the ventricles to further enable additional segmentation by latero-lateral composition (left, septal and right region). Existing endocardial and subendocardial ROIs were automatically assigned to the respective side. Sub-discrimination of myocardial, subepicardial and epicardial ROIs required the construction of additional lines that were then used to divide the tissue into left and right side, with the remainder being attributed to the septum area. Data from both the concentric and the latero-lateral segmentation were finally combined to create a third, more detailed set of ROIs. Independent of the segmentation, ring-shaped perivascular collagen was identified for later optional exclusion from quantification. Visualizations of all three segmentation dimensions were saved and all generated ROIs were exported as .zip-files to facilitate later collagen analysis without having to repeat the segmentation process beforehand. However, quantification can also be performed subsequently after segmentation, resulting in output parameters measured separately for each previously defined ROI region and saved as .csv and/or .xlsx-files.

Input parameters

In order to control the different functions the *QuantSeg* macro offers and to define the parameters needed to perform both segmentation and analysis, an initialization file was designed to be read by the macro at the beginning of each run. After specifying its location directly in the source code, users can freely configure the macro to their needs. Its use is obligatory as it contains fundamental parameters such as the ventricular dimensions *QuantSeg* should look for when segmenting, thickness values used for delineating different strata, thresholds essential for collagen recognition, as well as options related to the creation of visualization images. Along with detailed explanations of every parameter, the file is available in the [supplementary material](#).

Method validation

To confirm that this new method is at least equivalent to other commonly used techniques, a set of murine heart sections was analyzed using the fluorescence microscopy-based technique in addition to the color hue-based approach described above, and *Collagen Score* and *Area Fraction* values were compared. In order to further validate the capabilities of the segmentation feature, a small number of rat hearts with myocardial infarction—displaying segmental, transmural fibrosis—were used.

Fluorescence microscopy

PSR stained slides were imaged using the same BZ-X810 microscope by KEYENCE, this time in fluorescence mode. Using a 20X objective lens, images were acquired using both the GFP filter for the parenchyma and the TexasRed filter for collagen. For detailed information regarding equipment and wavelengths, please refer to the [supplementary material](#). Due to the high fluctuations in fluorescence intensity, fixed exposure times could not be used and needed separate manual adjustment for each image. For the collagen channel, vascular collagen was taken as a reference to calibrate exposure time. After acquisition, tile images were stitched as described previously.

Fluorescence image analysis

Analysis of fluorescence images was performed using another short FIJI macro, hereafter referred to as the “fluorescence macro”. First, pixels representing areas of unspecific fluorescence—characterized by persistent signal in both channels at the same time—were removed by subtracting the green from the red channel using absolute values. Second, using brightness thresholds, collagen and cardiomyocytes were selected in their respective channel after which area and mean gray value were saved. A *Collagen Score*—calculated as described below—was then displayed alongside the fractional area. Due to the strong variation in collagen content and fluorescence intensity, the brightness threshold had to be chosen manually by the user to guarantee a reasonable selection of the structures of interest. The code of the fluorescence macro can be found in the [supplementary material](#).

Statistics

All statistical analyses were performed using GraphPad Prism version 10.1.0 for Windows, GraphPad Software, Boston, Massachusetts, USA, www.graphpad.com. Because most of the data were found to be distributed log-normally, values were first transformed using the formula $Y = \ln(Y)$. The resulting data then passed normality tests required for ANOVA; additionally, QQ plots appeared straightened afterward. Diagrams show the mean and SEM along non-transformed values within a logarithmic coordinate system in order to better visualize statistical results. In cases in which no prior transformation was used, linear axes are depicted. ****: $p < .0001$; ***: $.001 > p > .0001$; **: $.01 > p > .001$; *: $.05 > p > .01$.

Results

General principles of the novel *QuantSeg* macro

To minimize the need for technical equipment such as special microscopes or trained personnel, the collagen quantification part of the *QuantSeg* macro was based on the evaluation of color hue and saturation in BF images which can be acquired using any light microscope with digital capabilities. For best results, it is recommended to capture higher magnification tile images and to perform stitching afterward using software. To ensure a high

degree of objectivity and speed of analysis, we developed an algorithm that takes overview images of entire heart sections and processes them as a whole without the need of frequent user intervention. The program was designed to be strictly deterministic, meaning that for one image, the same results will be produced on repeated analysis runs, guaranteeing additional inter-user reliability.

All parameters that control the features active in any analysis run can be chosen freely beforehand in the initialization file, saving run time when disabling steps that are not needed at the time. Threshold values that form the basis of collagen recognition have to be set here, as well, as they are strongly dependent on the exact hues produced by the staining, color saturation, exposure time, and other factors.

In general, *QuantSeg* converts one image of a heart section into a set of numerical result parameters, as well as images that visualize collagen recognition or heart segmentation. The extent of numerical outputs depends on the dimensions of segmentation chosen within the initialization file. For visualizations, sketches can be produced that schematically show the borders between regions within different segmentations (Fig. 1 A–C). Furthermore, a false-color representation of the recognized collagen can be produced. In this depiction, the thresholded a*-channel is mapped to the lookup table (LUT) “Fire” and superimposed over

the grayscale saturation channel, clearly highlighting the collagen recognized in the image against the parenchymatous background (Fig. 1D).

The leading parameter *Collagen Score* does not only consider the parenchymal and collagenous regions, but also accounts for color intensity values of both. Mathematically, this result is without unit. However, we decided to introduce the unit “Collagen to Parenchyma Ratio”, abbreviated CPR. To account for the fact that most of the time, the resulting values are very small and are therefore multiplied by 1000 by default, the letter “m” is added to the unit’s name. Further explanations and formulas underlying the output values are listed in [Supplementary Table 1](#). Numerical results can be written into a .csv or an .xlsx file, the latter requiring the external FIJI plugin *Read and Write Excel* [17]. Visualizations can be saved optionally, either as TIFF or JPEG files.

Comparison of *QuantSeg* and fluorescence data

In order to validate and compare our new quantification method to the conventional fluorescence macro described above, representing an established, commonly used technique, we used PSR-stained heart sections of *Jup*-KO mice compared to WT littermate controls. BF and fluorescence images were captured using the same fluorescence microscope (BZ-X810, KEYENCE). [Figure 2A](#)

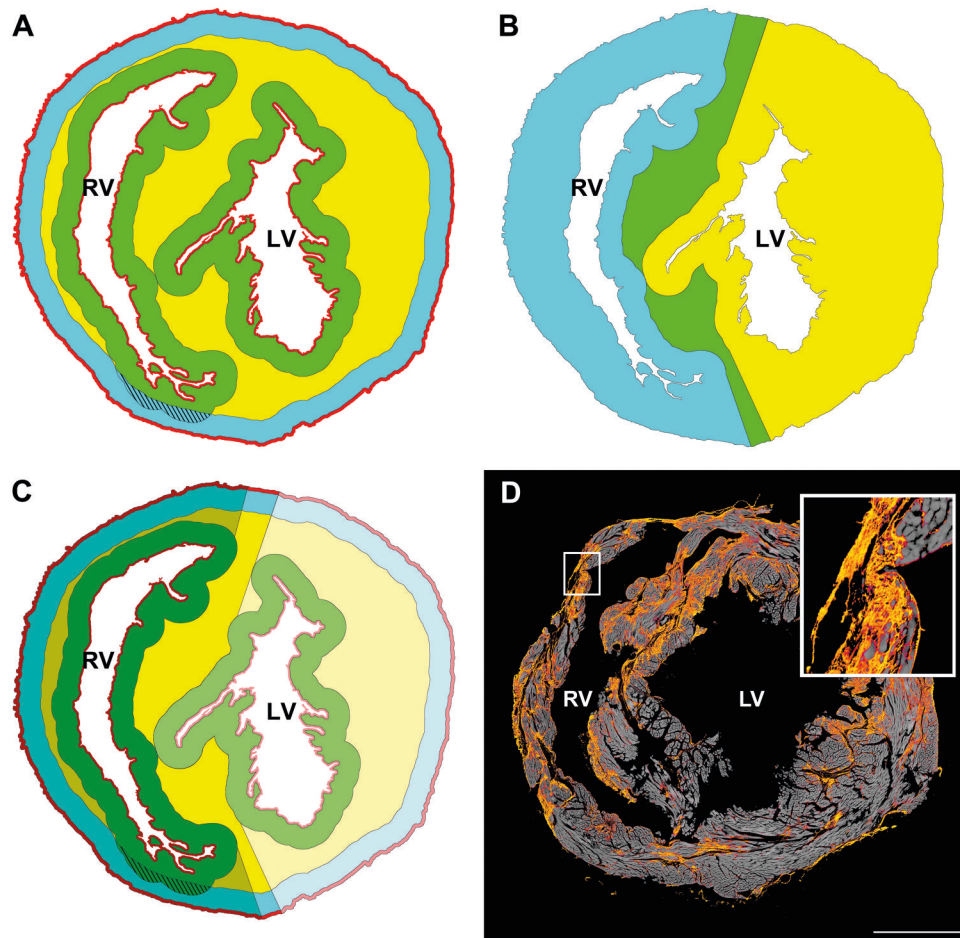


Figure 1. Optional visualization images put out by the macro. Segmentation by concentric wall layers (A), laterolateral composition (B), or both combined (C). Crosshatching shows overlap of regions. Darker areas in (C) indicate right heart, medium areas septum, and light ones left heart. The sketches are representations of the section shown in [Fig. 2B](#). Labeling of ventricles in sketches is done automatically by *QuantSeg*. False-color representation (D) highlighting collagen in the heart section shown in [Fig. 2A](#). Rectangle represents zoomed inlay. Scale bar: 1000 μ m. Abbreviations: LV: left ventricle, RV: right ventricle.

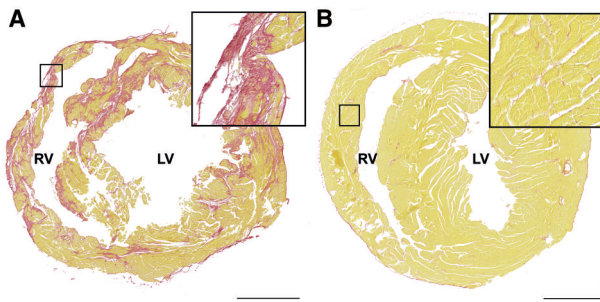


Figure 2. Representative PSR-stained heart sections of 8-week-old animals. *Jup*-KO mouse heart displays extensive fibrosis and myocardial atrophy (A). WT control mouse heart tissue without fibrosis, representing the aspect of a healthy heart with normal collagen content (B). Stitched overviews. Scale bars: 1000 μ m. Rectangles represent zoomed inlays. Abbreviations: See Fig. 1.

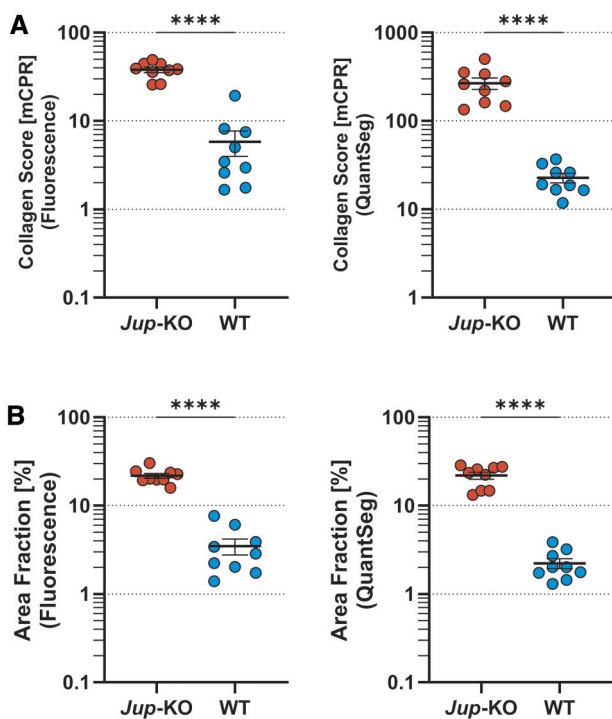


Figure 3. Scatter plots showing collagen content determined using the conventional fluorescence technique compared to the *QuantSeg* macro. The same hearts from 6–8-week-old animals were analyzed using both methods. *Collagen Score* (A) and *Area Fraction* (B) represent both methods' main output parameters. Statistics performed by two-tailed unpaired t-test with (A) and without (B) Welch's correction. $n = 9$.

shows a representative *Jup*-KO heart section with extensive interstitial and disseminated fibrosis located in both ventricular walls and the septum, comprising subepicardial, myocardial, as well as endocardial areas. Figure 2B shows a representative WT heart without *Jup* deficiency, displaying physiological amounts of collagen located predominantly around blood vessels as well as in the epi- and endocardium.

In BF images, analysis was performed with the new *QuantSeg* macro and in fluorescence images using the fluorescence macro. Both methods were able to detect the significant difference in collagen content between *Jup*-KO and WT hearts, for both *Collagen Score* and *Area Fraction* ($P < .0001$, Fig. 3A). The mean of *Area Fraction* obtained from the *QuantSeg* macro analysis proved to be very close to the one resulting from fluorescence analysis

(Fig. 3B). Value dispersion, however, was visibly greater in the fluorescence data for low collagen content WT hearts. Supplementary Table 2 displays the coefficients of variation for all groups of Fig. 3, clearly showing more closely grouped values around the mean for WT hearts from *QuantSeg* analysis compared to those obtained via the fluorescence-based technique. *QuantSeg* produced only slightly larger value dispersion in high collagen content hearts.

More comprehensive understanding of fibrosis patterns

As already stated, apart from the two parameters indicating a general degree of fibrosis within the tissue, the *QuantSeg* macro provides more information concerning distribution of collagen and the resulting patterns of fibrosis. However, no significant differences in mean ($P = .0747$, Fig. 4B) or max collagen color intensity ($P = .8745$, Fig. 4C) were detected between *Jup*-KO and WT hearts, indicating that differences in degree of fibrosis do not stem from discrepancies in color saturation. Furthermore, no significant differences in tissue density ($P = .0899$, Fig. 4F) were found. For parameters regarding different fibrosis patterns, however, a significantly larger total area of collagen ($P < .0001$, Fig. 4A), mean collagen spot area ($P < .0001$, Figure 4D), and number of collagen spots ($P < .0001$, Fig. 4E) were observed in *Jup*-KO samples. These results show that the differences depicted in Fig. 3 are caused by significantly more numerous and larger collagen spots that lead to an overall increase in area encompassed by collagen.

Segmented collagen quantification in *Jup*-KO hearts

In order to quantify the collagen content in the different micro-anatomical regions within a heart section, a full segmentation of each of the same hearts was performed, followed by a differentiated collagen analysis using the *QuantSeg* macro. Parameters used for segmentation can be found in the initialization file within the supplementary material. Across all regions analyzed, a strong difference between *Jup*-KO and WT hearts was detected, both for *Collagen Score* and *Area Fraction*. When comparing group means, all regions belonging to laterolateral composition were equally affected by fibrosis in *Jup*-KO compared to WT mice for both *Collagen Score* and *Area Fraction* ($P < .0001$, Fig. 5A). Regarding segmentation into concentric wall layers, differences were also prominent in all layers ($P < .0001$, Fig. 5B), with myocardial tissue from *Jup*-KO displaying a higher fraction of fibrotic areas than the associated serous membranes (endo- and epicardium). The results indicate that here, a disseminated pattern of fibrosis is present, with all regions of the heart contributing to the differences seen in the overall collagen content.

Segmented collagen quantification in MI rat hearts

Rat hearts with experimental MI by means of ligation of the left anterior descendant coronary artery and therefore transmural, segmental fibrosis (Fig. 6A), were analyzed to better demonstrate the capabilities of the *QuantSeg* macro's segmentation feature. Sham-treated littermates served as controls (Fig. 6B). MI hearts showed a significantly higher *Collagen Score* compared to sham ($P = .0012$; Fig. 7A). For both *Collagen Score* and *Area Fraction*, the segmented collagen quantification showed a more or less unaffected right heart and septum, in contrast to a significantly increased collagen content located in the left heart ($P < .0001$, Fig. 7B). Here, the evaluation of concentric fibrosis pattern is not

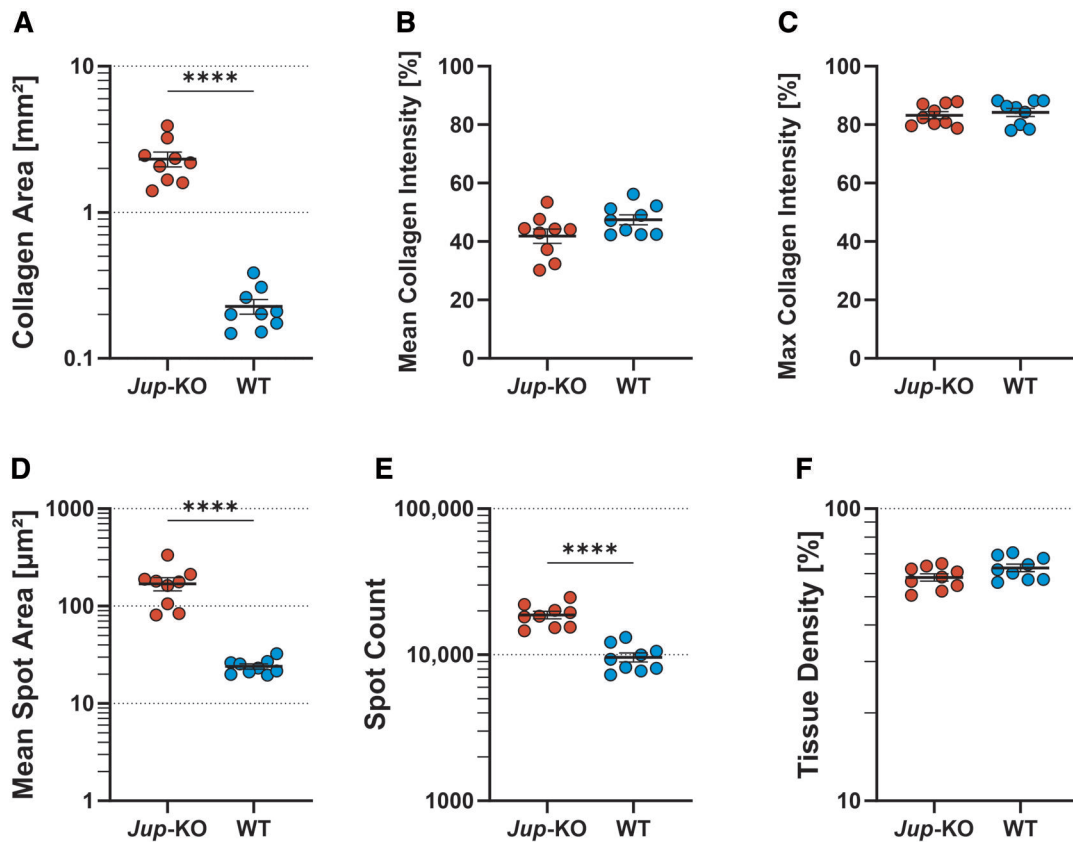


Figure 4. Scatter plots showing additional *QuantSeg* output parameters. Significant differences in Total Collagen Area (A), Mean Collagen Spot Area (D), and Number of Collagen Spots (E). No differences in Mean (B) and Maximum (C) Collagen Intensity and Tissue Density (F). The same hearts from 6–8-week-old animals were analyzed. Linear axes were used in (B, C). Statistics performed by Mann–Whitney test (A) or two-tailed unpaired t-test with (D) or without (B, C, E, F) Welch’s correction. $n = 9$.

expedient as following the MI, the left ventricular wall has thinned considerably so that the micro-anatomical boundaries cannot be established adequately by the segmentation algorithm.

Discussion

The main goal of our work was to develop and provide a method for analyzing whole PSR-stained histological sections that is quick, easy, and more powerful than previous approaches while being reproducible, objective, robust, cheap, and freely available, all at the same time. It was of major importance to obtain results that can be compared even across staining batches and different experiments. Furthermore, we wanted to expand the possibilities of this technique by enabling micro-anatomically differentiated quantification of the collagen content in heart sections. To achieve this, an extensive macro for the software FIJI was developed and tested.

Comparability to established methods

Our novel *QuantSeg* macro was able to quantify the difference in collagen content between fibrotic and healthy hearts just as well as the fluorescence microscopy-based method. In hearts with low collagen content, *QuantSeg*-derived data were even more robust and showed less value dispersion. This can most likely be accounted to problems in delimiting collagenous areas those sections using the fluorescence-based approach as we observed that choosing valid image acquisition and analysis parameters proved

extremely difficult. Due to the strong variance of fluorescence in different sections, it was necessary to manually and often drastically adjust exposure times in order to maintain comparable levels of signal. An additional bias was caused by the need to threshold manually, further introducing subjectivity into the results. Even small adjustments resulted in large alterations for the area counted as collagen. Furthermore, the signal intensity of the tiny amount of collagen present in the tissue was comparable to that from non-specific red background, which made a clear differentiation very hard. Organs with high amounts of fibrosis, on the other hand, usually displayed strong red fluorescence clearly discernable from background, simplifying threshold selection. BF images of the same organs proved to be more consistent which is why in most cases, the same thresholds can be applied throughout. In addition, BF images do not contain non-specifically stained structures or background signal, rendering this acquisition mode more suitable for accurate collagen quantification.

Advantages of *QuantSeg*’s collagen quantification feature

Rather practical advantages of this method lie in the staining and imaging techniques needed. Because the macro is built on the interpretation of BF images, the requirement for expensive and highly specialized equipment such as fluorescence or polarization microscopes is eliminated [3–5]. Also contributing to the affordability of this method is that (i) no paid or proprietary programs are used and (ii) no specialized training regarding

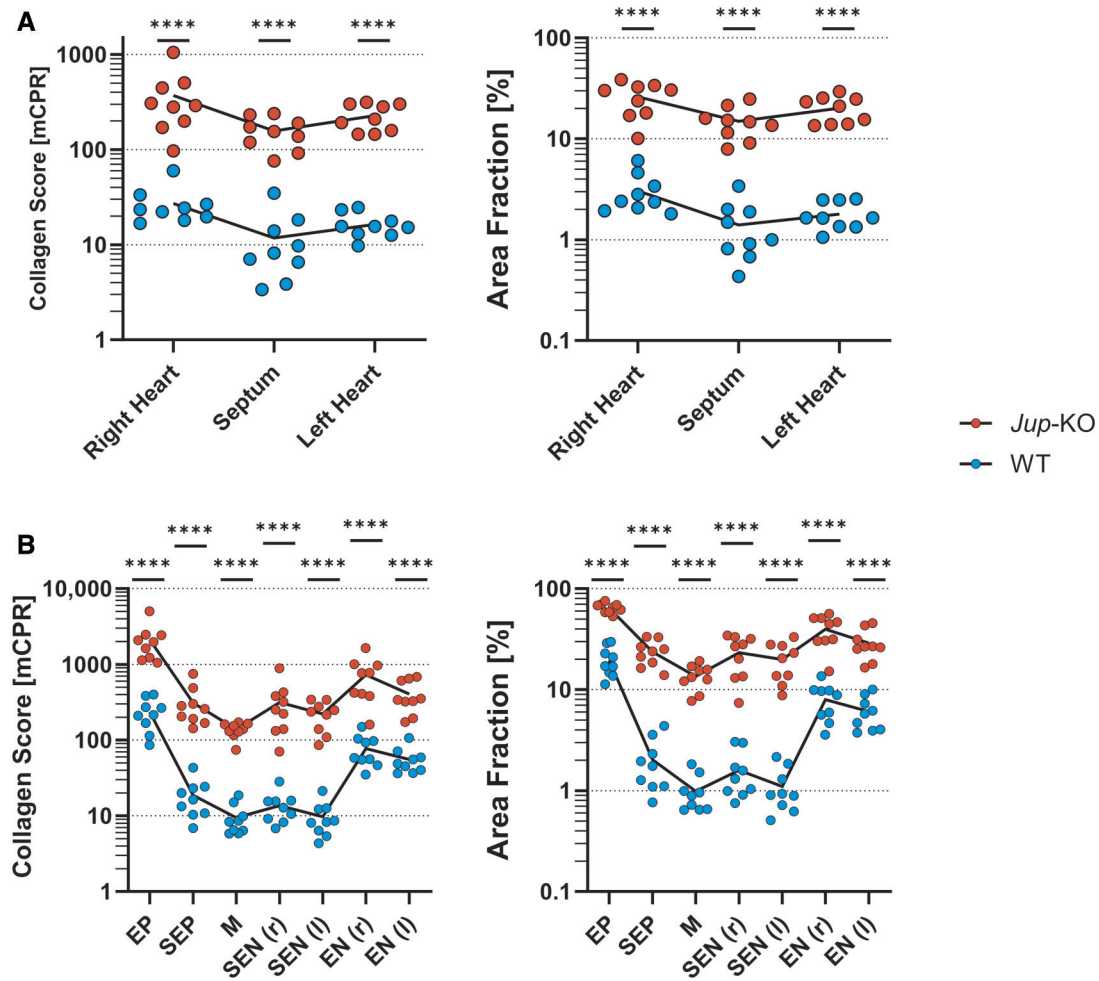


Figure 5. Scatter plots showing data from segmented collagen quantification. PSR-stained heart sections from 6–8-week-old animals were segmented in two dimensions [latero-lateral composition (A), strata (B)] and analyzed using the macro. Statistics were performed by two-way ANOVA and Šidák's multiple comparisons test. $n = 9$. Abbreviations: EP: epicardium, SEP: subepicardial layer, M: myocardium, SEN: subendocardial layer, EN: endocardium, (r): right ventricle, (s): septum, (l): left ventricle.

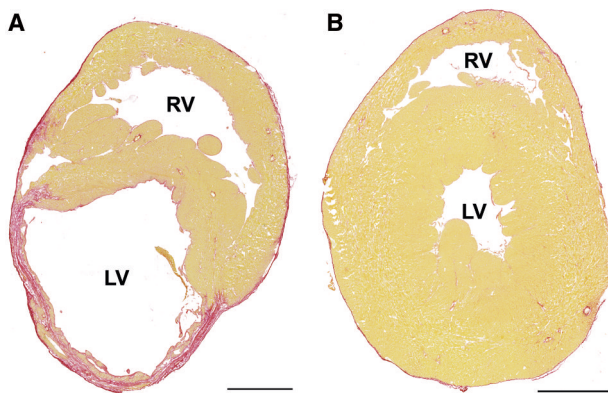


Figure 6. Representative PSR-stained rat MI and sham heart sections. 8 weeks after MI rat hearts displayed strong, segmental, left-ventricular fibrosis and myocardial atrophy (A). 8 weeks after sham procedure, control rats represented healthy hearts with normal collagen content (B). Stitched overviews. $n = 3$. Scale bars: 2500 μm . Abbreviations: See Fig. 1.

equipment or software is required. Due to its speed, the technique is easily scalable to large numbers of images: In contrast to fluorescence microscopy, image acquisition times are lower due

to shorter exposure times and only one channel being imaged. Whole sections can be processed at once, eliminating the need for repeated capture and analysis of singular view frames from the same slide. The usage of BF images also ensures a high degree of inter-user reliability because usually, one and the same exposure time and white balance setting can be used for an entire batch of slides with no need of constant intervention or manipulation. Employment of microscopes with automation features even allows for largely unattended image acquisition. The high reliability and robustness of the quantification algorithm also allows for better comparison of data from different experiments.

Furthermore, only one program is used throughout the entire quantification process. Analysis times therefore range from roughly 15 s to 2 min per image, depending on its resolution and the enabled features, clearly setting it apart from manual methods. Direct speed comparisons to other computational methods were not possible due to their limited availability. Also, for the analysis process a minimal amount of user decisions has to be made: As long as staining intensity and color hues are constant among the images, the threshold values necessary for analysis need to only be set once at the beginning and kept throughout an entire batch. Apart from that, users are only required to open the respective images within Fiji and start the macro, ensuring a very high degree of objectivity and reproducibility. Regarding the

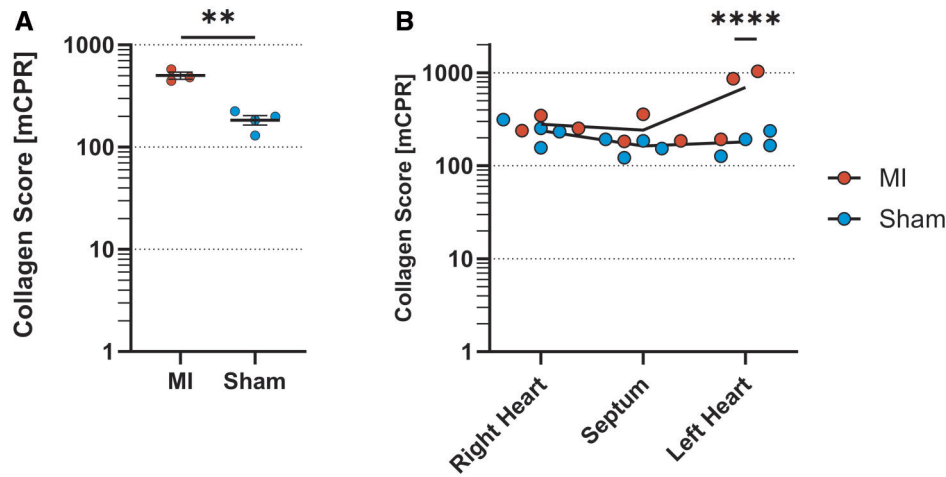


Figure 7. Collagen quantification of MI rat hearts with and without prior segmentation. Hearts from rats with and without myocardial infarction were examined using the *QuantSeg* macro. Scatter plot shows overall collagen content of MI vs. sham hearts (A). Statistics performed by two-tailed unpaired t-test. Line plots show data from collagen quantification segmented by latero-lateral composition (B). Statistics were performed by two-way ANOVA and Šidák's multiple comparisons test. $n = 3$. Abbreviations: See Fig. 5.

output of results, this method offers a more comprehensive set of parameters measured than most methods: *Collagen Score* (incorporating color intensity), *Area Fraction*, *Collagen Area*, *Mean Collagen Intensity*, *Max Collagen Intensity*, *Mean Spot Area*, *Spot Count*, and *Tissue Density* allow for broader conclusions compared to other computational methods, also regarding patterns of fibrosis. The automated output into tabular files greatly reduces the risk of manual transcription errors.

Apart from that, polarization imaging is known to have limitations in its sensitivity when visualizing very thin or disorganized fibrils, such as in reticular collagen type III or basement membranes containing collagen type IV. Most of the time, those structures are better appreciated in PSR-stained BF images given their strong red staining [18].

Limitations of the collagen quantification feature

As differentiation of collagen and parenchyma is highly dependent on color intensity and hue, a high quality and consistency of staining is critical for the successful employment of this method. Although the time span between staining and analysis when using BF imaging and the *QuantSeg* macro is of low importance due to the high temporal stability of PSR staining, results can be influenced by varying quality of fixation and embedding, section thickness, staining time, as well as diluted or contaminated staining solutions [3]. *QuantSeg* does not have the capability to alert the user to such problems or even correct for them. Thus, quality and consistency of staining must be ensured. Also, one should verify that data generated by *QuantSeg* matches visual assessment of samples in question. Furthermore, failure to properly white balance before image acquisition has the potential to strongly distort results despite the macro's internal white balancing efforts. This is because those are done on an image exhibiting a compressed color depth of 24-bit, possibly yielding different hues after white balancing than the microscope sensor would produce. Fluorescence and polarization microscopy-based methods are less vulnerable to that as both fluorescence signal as well as birefringence ensure a high specificity in recognizing and delineating collagenous areas by means less dependent on those factors. In addition, differentiation of collagen fiber thickness and packing density is lost with BF imaging as this feature is only achievable with polarization microscopy [19]. The *QuantSeg*

macro therefore does not offer means to automatically exclude the non-collagen structures mentioned above from the analysis that are stained red by PSR. If the tissue to be analyzed is at risk of containing such structures, employment of a polarization-based or histochemical method should be considered instead. Regarding the *Collagen Score* output parameter, color intensity values (from 0 to 255) for collagen and parenchyma are included into the calculation. On the one hand, this allows for a better differentiation of sections that might exhibit comparably large areas of collagen yet differ in color intensity. Also, higher levels of color intensity in general (e.g. through longer staining times) are automatically corrected for by dividing the product of collagen area and saturation by the saturation of parenchymal tissue. The exact influence of these parameters of color saturation is not known which is why *Collagen Score* values should be critically evaluated pertaining to this possible bias. On the other hand, so far, it is not known if and how density, thickness, type, or orientation of collagen fibers influence red saturation in PSR-stained sections and whether it changes linearly with just one, or exponentially with multiple of these parameters. This poorly understood relationship could lead to higher value dispersion especially in regions with low collagen content as shown in [Supplementary Table 2](#). Therefore, the interpretation of *Collagen Score* values should be done with respect to this fact, too. If these characteristics are of particular interest, polarization-based methods should be used instead. Another problem could be that tissues with very high degrees of fibrotic scarring and atrophy can present paler in color than less affected counterparts in some cases. Causes for this might be decreased density of the tissue, pseudo-vacuoles, and high content of non-collagenous extracellular matrix. Intuitively, one might want to assign a higher fibrosis score to those areas, but, due to their paleness, the *QuantSeg* macro will output lower *Collagen Score* and also *Area Fraction* values, through under-recognition of non-parenchymal areas in this case. Similarly, *QuantSeg*'s reliability when analyzing samples of very low collagen content proved superior to the fluorescence-based approach yet was not tested extensively. For those cases, hydroxyproline assays such as the one developed by Lin and Kuan (2010) might be more suitable as it exhibited a very low detection limit [10]. Furthermore, *QuantSeg*'s reliability when quantifying collagen in hearts of different species or other types

of tissue is unknown because it was only tested on murine cardiac tissue within this study. Therefore, users must be especially careful in interpreting data generated in such contexts and should ensure validity of results beforehand. The same is true for non-formalin-fixed paraffin-embedded tissue.

Capabilities analyzing collagen distribution patterns

Without performing segmentation, output values like *Collagen Area*, *Mean Spot Area* or *Spot Count* can give information about the general collagen distribution pattern. In case of the *Jup*-KO hearts analyzed above, these values show that their higher *Collagen Score* can be attributed not only to a significantly higher mean area of collagen spots, but also to a higher number of them, leading to an overall increase of collagen area. In cases in which different patterns (e.g. few big spots vs. numerous small ones) would produce comparable *Collagen Scores*, looking at these values can unmask those differences. To obtain even more information about the spatial distribution of cardiac collagen, the powerful, optional segmentation feature of the macro can be used to automatically recognize different micro-anatomical regions in a section on each of which a separate collagen quantification can then be applied. The data at hand gives two examples for how this feature can be used. First, segmented analysis expands the information obtained about *Jup*-KO hearts by showing that, although no single region outstandingly contributes to the high *Collagen Scores*, parenchymal areas are more strongly affected by fibrosis than the serous membranes (epicardium, endocardium). Still, a significant increase in epicardial and endocardial collagen can be seen which is surprising considering that the JUP-deficiency in this model is cardiomyocyte specific. In hearts affected by artificial MI, on the other hand, one region responsible for the difference in *Collagen Scores* can be clearly identified. Here, the left side of the heart is the only region with significant fibrosis, due to the prior artificial occlusion of the left coronary artery. Analyses like these previously had to be performed by capturing individual, high-magnification view-frames from manually identified regions of the heart, quantifying them one by one and averaging afterward. Such technique could have produced similar results here but image acquisition and analysis time would have been many times larger. When high quality and intact sections are used, segmentation is fully automatic which further eliminates sources for errors, subjectivity and thereby data dispersion.

Limitations of heart segmentation

This feature was developed for and, so far, tested diligently on transverse murine heart sections. For it to work properly, it is mandatory that the heart sections are of high quality and retain important morphological features throughout the fixation, sectioning, and staining process. The macro does not possess any capabilities in recognizing areas that are superior to the users' ones. In case the anatomy of a section is unrecognizable to humans, the macro will most likely not be able to produce a sensible segmentation either. Theoretically, the segmentation feature should be applicable to longitudinal sections in which both ventricles are clearly distinguishable, as well. A known issue here concerns the segmentation into left, septal and right heart. In this case, the part of the algorithm generating the straight separation lines within the tissue often malfunctions due to the bi-convex shape of longitudinally sectioned ventricles: In transverse sections, right and left ventricles are often shaped more convex-concave and round, respectively. The algorithm was adjusted specifically for this morphology and therefore can produce

questionable results or even crash when presented with majorly differing ventricle shapes. Similar problems might arise when segmenting hearts of different species. In general, though, cardiac tissue sections from animals other than mice or rats should not pose a problem. However, as soon as the anatomy of the sample is not comparable to that of murine hearts, sensible segmentations might not be produced. In case of two-chamber fish hearts, the attribution of left and right ventricle will fail or at least output nonsensical results while, additionally, the looser packaging of cardiomyocytes could interfere with the recognition of ventricles. Users should test whether segmentation works on the samples beforehand and, if necessary, consider modifying sectioning accordingly.

An inevitable consequence of making the thickness of epicardium, subepicardium, subendocardium, and endocardium freely adjustable by the user is that in some cases, one and the same area can be attributed to more than one anatomical region. In case of the junction area between a thin right ventricular wall, thin septum, and thin left ventricular wall, this area could be considered subendocardium, subepicardium, right, and left heart all at the same time. This effect could influence results especially in hearts exhibiting myocardial atrophy, which leads to wall thinning. However, such an overlap can be reduced by decreasing the respective layer thicknesses in the initialization file. The *QuantSeg* macro is strictly deterministic, meaning it produces the same results on repeated runs as long as the same parameters are used. Therefore, segmentations only represent estimations of where micro-anatomical boundaries might be located. Those results are in no way universal or represent a "ground truth". They are strongly dependent on the layer thickness settings, the morphology of the section, as well as the methodology that is inherent to the code. Data generated using this feature should be verified and interpreted with respect to this.

Conclusion

The data presented provide a first indication that the method described here can be used as a valid technique in analyzing PSR-stained cardiac tissue sections with notably superior capabilities in detecting subtle differences between specimens with overall low collagen content. Its affordability, quickness, ease of use, objectivity, and multitude of output parameters let it stand out from other available methods and bear the potential to render time-consuming in-house solutions and tedious manual approaches obsolete. In the future, larger-scale employment and testing of *QuantSeg* is needed to confirm its envisaged broad usability and establish it as an accepted and validated technique.

Acknowledgements

We thank Paula Arias-Loza, PhD, for providing histology sections of rat hearts and Susanna Schraut for technical assistance.

Supplementary data

Supplementary data are available at *Biology Methods and Protocols* online.

Conflict of interest statement. None declared.

Author contributions

Julian Kammerer (Data curation [lead], Methodology [lead], Software [lead], Validation [equal], Visualization [equal], Writing—original draft [lead]), Alexandra Cirnu (Data curation [equal], Methodology [equal], Validation [equal], Visualization [equal]), Tatjana Williams (Data curation [supporting], Supervision [equal], Writing—review & editing [supporting]), Melanie Hasselmeier (Data curation [equal], Investigation [equal], Validation [equal]), Mike Nörpel (Data curation [supporting], Formal analysis [supporting], Investigation [supporting], Validation [supporting]), Ruping Chen (Supervision [equal], Validation [equal], Writing—review & editing [equal]), and Brenda Gerull (Conceptualization [lead], Funding acquisition [lead], Project administration [lead], Supervision [lead], Writing—review & editing [lead])

Funding

This work was supported by the German Research Foundation (DFG; SFB 1525; project number: 453989101; to B. Gerull). J. Kammerer was supported by a scholarship of the Graduate School of Life Science (GSLs), Würzburg. M. Nörpel received the Otto-Hess-Scholarship of the German Society of Cardiology (DGK).

Data availability

The data underlying this article are available in its online [supplementary material](#).

References

- Sweat F, Puchtler H, Rosenthal SI. Sirius Red F3BA as stain for connective tissue. *Arch Pathol* 1964;**78**:69–72.
- Constantine VS, Mowry RW. Selective staining of human dermal collagen: II. The use of picosirius red F3BA with polarization microscopy. *J Invest Dermatol* 1968;**50**:419–23. <https://doi.org/10.1038/jid.1968.68>
- Junqueira LCU, Bignolas G, Brentani RR. Picosirius staining plus polarization microscopy, a specific method for collagen detection in tissue sections. *Histochem J* 1979;**11**:447–55. <https://doi.org/10.1007/BF01002772>
- Dolber PC, Spach MS. Conventional and confocal fluorescence microscopy of collagen fibers in the heart. *J Histochem Cytochem* 1993;**41**:465–9. <https://doi.org/10.1177/41.3.7679127>
- Whittaker P, Kloner RA, Boughner DR et al. Quantitative assessment of myocardial collagen with picosirius red staining and circularly polarized light. *Basic Res Cardiol* 1994;**89**:397–410. <https://doi.org/10.1007/BF00788278>
- Rich L, Whittaker P. Collagen and picosirius red staining: a polarized light assessment of fibrillar hue and spatial distribution. *Brazilian Journal of Morphological Sciences* 2005;**22**:97–104.
- Hadi AM, Mouchaers KT, Schaliq I et al. Rapid quantification of myocardial fibrosis: a new macro-based automated analysis. *Cell Oncol (Dordr)* 2011;**34**:343–54. <https://doi.org/10.1007/s13402-011-0035-7>
- Vogel B, Siebert H, Hofmann U et al. Determination of collagen content within picosirius red stained paraffin-embedded tissue sections using fluorescence microscopy. *MethodsX* 2015;**2**:124–34. <https://doi.org/10.1016/j.mex.2015.02.007>
- Courtoy GE, Leclercq I, Froidure A et al. Digital image analysis of picosirius red staining: a robust method for multi-organ fibrosis quantification and characterization. *Biomolecules* 2020;**10**:1–23. <https://doi.org/10.3390/biom10111585>
- Lin Y-K, Kuan C-Y. Development of 4-hydroxyproline analysis kit and its application to collagen quantification. *Food Chem* 2010;**119**:1271–7. <https://doi.org/10.1016/j.foodchem.2009.08.009>
- Schindelin J, Arganda-Carreras I, Frise E et al. Fiji: an open-source platform for biological-image analysis. *Nat Methods* 2012;**9**:676–82. <https://doi.org/10.1038/nmeth.2019>
- Rueden CT, Schindelin J, Hiner MC et al. ImageJ2: ImageJ for the next generation of scientific image data. *BMC Bioinformatics* 2017;**18**:529. <https://doi.org/10.1186/s12859-017-1934-z>
- Shoykhet M, Trenz S, Kempf E et al. Cardiomyocyte adhesion and hyperadhesion differentially require ERK1/2 and plakoglobin. *JCI Insight* 2020;**5**:1–15. <https://doi.org/10.1172/jci.insight.140066>
- Schinner C, Erber BM, Yeruva S et al. Stabilization of desmoglein-2 binding rescues arrhythmia in arrhythmogenic cardiomyopathy. *JCI Insight* 2020;**5**:1–16. <https://doi.org/10.1172/jci.insight.130141>
- Schinner C, Vielmuth F, Rötzer V et al. Adrenergic signaling strengthens cardiac myocyte cohesion. *Circ Res* 2017;**120**:1305–17. <https://doi.org/10.1161/CIRCRESAHA.116.309631>
- Arias-Loza PA, Hu K, Frantz S et al. Medroxyprogesterone acetate aggravates oxidative stress and left ventricular dysfunction in rats with chronic myocardial infarction. *Toxicol Pathol* 2011;**39**:867–78. <https://doi.org/10.1177/0192623311410441>
- ImageJ Wiki. Read and write Excel. <https://imagej.net/plugins/read-and-write-excel> (October 10, 2022, date last accessed)
- Dapson RW, Fagan C, Kiernan JA et al. Certification procedures for sirius red F3B (CI 35780, Direct red 80). *Biotech Histochem* 2011;**86**:133–9. <https://doi.org/10.3109/10520295.2011.570277>
- Dayan D, Hiss Y, Hirshberg A et al. Are the polarization colors of Picosirius red-stained collagen determined only by the diameter of the fibers? *Histochemistry* 1989;**93**:27–9. <https://doi.org/10.1007/BF00266843>

© The Author(s) 2024. Published by Oxford University Press.

This is an Open Access article distributed under the terms of the Creative Commons Attribution-NonCommercial License (<https://creativecommons.org/licenses/by-nc/4.0/>), which permits non-commercial re-use, distribution, and reproduction in any medium, provided the original work is properly cited.

re-use, please contact journals.permissions@oup.com

Biology Methods and Protocols, 2024, 00, 1–10

<https://doi.org/10.1093/biomethods/bpae027>

Methods Article

For

commercial